Enhanced Biological and Photo catalytic activity of polypyrrole-$BiVO_4$ nanocomposite

[1]T. Shapter Hasmi, [2]T. Pradeep, [3]M.Sangareswari*

Inorganic and physical chemistry laboratory, CSIR-CLRI, Adyar, Chennai-600 020
Department of Physical chemistry, Madurai Kamaraj University, Madurai-625 021
Department of chemistry, S.M.S College of Arts and Science, Sivakasi- 626131

Abstract*: Photo catalytic degradation plays a significant role for the decomposition of organic pollutant in water since it is cost effective and environment-friendly. Semiconductor are the prominent choice for the photo catalytic degradation that exhibits remarkable activities upon ultra violet (UV) light irradiation and fails to utilize the maximum part of the solar spectrum *i.e.* visible light fraction. Bismuth vanadate ($BiVO_4$) has recently attracted much attention as one of the Ti–free photo catalysts suitable for visible light photo catalytic degradation. Unfortunately, its quick recombination of charge carriers, poor adsorption capacity, and critical drawback of photo corrosion are pulling the researchers to think about suitable modification of the $BiVO_4$. In this exertion, we attempted here to improve the adsorption capacity and visible light driven photo catalytic activity of $BiVO_4$ towards methylene blue (MB) by combining with electron donating organic polymer polypyrrole (PPy). This PPy-$BiVO_4$ nanocomposite was synthesized using chemical oxidative polymerization method and characterized by TEM, SEM-EDAX, XRD, UV-DRS, TGA, DTA and PL analysis. Photo catalytic experiments were performed using direct sunlight irradiation and the observed results show that the PPy-$BiVO_4$ nanocomposite degraded MB more efficiently than the pure $BiVO_4$. The photocatalytic dye degradation performance obtained in 75.8% for MB dye owing to the interaction between the catalyst and the MB dye. The another possible reason for that due to its enhanced surface area and electron transfer rate. The one more possible reason for that, same composition and similar energy structure which affected the photocatalytic activity of the prepared material under UV and Solar light irradiation, which was attributed to the distortion of the Bi-O polyhedron by $6s^2$ lone pairs of Bi^{3+}, the results indicated that the different distortion of the metal-oxygen polyhedron is another important factor affecting the photocatalytic activity via causing different elastic properties of the catalysts and affecting separation efficiency and dispersion of the photo-generated electrons and holes. Moreover, the PPy-$BiVO_4$ nanocomposite exhibits easy separation and less deactivation after several runs. It concludes that the new PPy-$BiVO_4$ nanocomposite acting as excellent photo catalyst for the decomposition of MB and it could be a potential candidate for essential waste water treatment.

***Keywords*: Polypyrrole; Bismuth Vanadate; Zero point charge; Adsorption; Visible light; Methylene Blue**

1. Introduction

Nowadays, the impact of the industrial toxic organic dyes and their effluents become one of the main sources of water pollution [1]. Especially, methylene blue (MB) has considerable attention as it is difficult to degrade and causes breathing difficulty, vomiting, diarrhea and nausea in humans [2]. Hence, it is essential to remove MB from water bodies to protect not only humans and also water based animals and plants. Several methods have been developed to remove MB from effluents including precipitation, adsorption, reverse osmosis, oxidation and reduction [3-7]. Unfortunately these methods are limited in terms of sludge formation, waste disposal and high operation cost, time consuming and ineffectiveness in cases where complicated aromatic compounds presented [8]. To overcome these limitations, photo catalytic degradation has been highly focused to remove such a dye and it is environment benign nature and cost effective.

Semiconductors are the primary choice for photo catalysis to decompose organic dyes using highly sustainable solar energy [9]. Titanium dioxide (TiO_2) is the most promising photo catalyst employing in various practical applications such as self-cleaning paints and window panes [10]. To date, TiO_2 is still undoubtedly the most efficient photocatalyst for the degradation of many organic compounds under UV light irradiation. However, TiO_2 is not ideal for all purposes and performs rather poorly in processes associated with solar photocatalysis because of its some following reasons; First, the photo-generated electrons in the CB of TiO_2 can recombine with the VB holes rapidly to liberate energy in the outward appearance of blocked heat or photons; Second, the decomposition of water into hydrogen and oxygen is a chemical reaction with large positive Gibb's free energy (ΔG = 237kJ/mol), thus the backward reaction (recombination of hydrogen and oxygen into water) easily proceeds; Third, the band gap of TiO_2 is about 3.2 eV. Since UV light only accounts for in the region of 4 % of solar energy, while visible light contributes about 50 %, the lack of ability to make use of visible light confines the effectiveness of TiO_2 in solar photo catalytic hydrogen production [11].

In order to make full use of solar energy, considerable efforts have been devoted to develop novel visible- light-driven photo catalyst during the past decades [12]. Recently, Bismuth containing nanostructures have been reported for their excellent photo catalytic activities under sunlight [15-20]. By this way, bismuth vanadate ($BiVO_4$) is one of the non-titania based visible light driven semiconductor photo catalyst [13]. Over the past few decades, $BiVO_4$ presented efficient photocatalytic capacity for the removal some organic components like 2-propanol, phenol, RhB and MB under Visible light irradiation. However, the activity of pure $BiVO_4$ is low due to its poor adsorptive performance and difficult migration of electron hole pairs [14]. To make $BiVO_4$ to show better photo catalytic activity, modification with polypyrrole (PPy) is an appropriate choice since it possesses unique electrical and photo sensitizers activity for absorbing Visible light. Further it contains an extensively conjugated π system and considered as a fine photo generated hole-transporting material, which is suitable to transfer electron and hole efficiently. In addition, PPy shows

good stability in acidic and neutral condition. In our earlier report we demonstrated that the presence of PPy monolayer molecules [ ]. To the best of our knowledge, the utilization of PPy to enhance the visible light photo catalytic activity of the $BiVO_4$ towards MB degradation is not reported yet.

The objectives of this study are four fold. The first objective involves the preparation of PPy-$BiVO_4$ nanocomposite by chemical oxidative polymerization method. The composites of PPy-$BiVO_4$ were prepared and characterized by TEM, SEM, XRD, TGA, UV-DRS, PL and FT-IR analysis. The second objective was to determine the effect of various operational parameters like Concentration, time, dose and pH were also investigated for the prepared PPy-$BiVO_4$ nanocomposite under Solar light irradiation. Among the various operational parameters pH plays a vital role for the degradation of MB dye. The pH variation depends upon the zero point of the prepared material. When the pH of the solution increases above 3 (pH>3) the % removal of dye was also increases. This is due to the surface charge of the catalyst. The third objective is to investigated the correlation studies between $BiVO_4$ and PPy-$BiVO_4$. The fourth objective is to study possible photocatalytic mechanism and also the stability of the photocatalyst under solar light irradiation.

2. Experimental

2 .1. Chemicals and Reagents

Pyrrole (Py) monomer (AR Grade) was purified twice under reduced pressure and stored at 0-4° C prior to use. Methylene Blue (MB) a typical azo dye, was used as the target pollutant in aqueous media to assess the photocatalytic activities of the PPy-$BiVO_4$ nanocomposites. Bismuth nitrate penta hydrate and Ammonium meta vanadate were purchased from Merck. All other reagents were analytical grade and were used as received.

2 .2. Synthesis of $BiVO_4$

The 0.1M Bi (NO_3). $5H_2O$ in 100 mL water and 0.1 M NH_4VO_3 in 100 mL in water, both solutions were mixed together in 100 mL solvent containing ethylene glycol and deionized water. Then the mixture was stirred for 1h at room temperature to get a yellowish solution. Afterwards, the mixture was exposed to high-intensity ultra sonic irradiation (600W, 20 kHz) at room temperature in ambient air for 2h. The obtained yellow precipitate was washed with DD water and absolute ethanol and then dried at 343k for 10h in air.

2.3. Synthesis of PPy-$BiVO_4$ nanocomposite

Suitable chemical oxidative polymerization of pyrrole was performed in the presence of negatively charged $BiVO_4$ nanoparticles using APS as an oxidant. A typical procedure is outlined: The 5 mmoL pyrrole was dissolved in 0.1M sulphuric acid solution. Then 200 mg of prepared $BiVO_4$ nanoparticles and 100 ml pyrrole solution were added into beaker. Then, it was kept under 5°C for 48hrs. Then 20 mL of APS solution was added drop by drop. The green coloured precipitate was obtained. Subsequently, the obtained product was washed with DD water to remove the residual ammonia solution. Finally the product was dried at room temperature overnight.

2.3. Instrumental analysis

UV-vis absorption spectra of the PPy-$BiVO_4$ nanocomposites were studied by UV-Visible spectrophotometer ("SHIMADZU" model: UV 2450). FT-IR spectra of the purified samples were measured using FT-IR spectrophotometer ["SHIMADZU" (Model: 8400S) spectrometer] to confirm the structural information. The thermal stability of the prepared samples was performed by TGA/DTA analyser [Japan model: TGA/DTA 6200]. The samples were heated from 30 to 800°C at a rate of 20°C min^{-1} in a nitrogen atmosphere. The crystallographic structures of the materials were determined by High resolution powder diffractometer (Model–RICH SIEFRT&CO with Cu as the X - ray source (λ=1.5406×10^{-10}m). The surface morphology of the sample was recorded using Scanning electron microscopy and energy dispersive X-ray analysis (SEM-EDAX) (Model: FEG Quantum 250 EDAX). TEM analysis was done by High Resolution Transmission Electron Microscopy (HRTEM) and Small Area Electron Diffraction (SAED) using FEI Tecnai F20 Transmission electron microscope to confirm the microstructure and morphology of the prepared sample. The photoluminescence measurements were performed in a luminescence spectrophotometer (Perkin-Elmer LS 45) operated at room temperature.

2.4. Evaluation of Photocatalysis

An aqueous solution of MB was used as a model contaminant for studying the adsorption performance and photocatalytic activity of the prepared materials. The initial MB concentration, C_i was 2 ppm. The adsorption experiments were performed by adding 50 mL of MB solution and 20 mg of photocatalyst in a 100 mL beaker, which can prevent the suspension from being irradiated by light. The suspension was kept in dark condition to attain adsorption-desorption equilibrium. After 30 min, the suspensions were kept in sunlight irradiation for 3hrs. A portion of samples were collected and centrifuged immediately for separation of any suspended solids. The change in the concentration of MB was monitored by measuring the absorbance at ($\boldsymbol{\lambda}_{max}$ = 665nm) with a UV-Vis spectrophotometer. The decolourization ratio of contaminant was calculated as follows:

$$\text{Percentage removal (\% R)} = \left[\frac{C_i - C_t}{C_i}\right] \times 100 \quad ----- \quad (2.1)$$

Where,

C_o- initial concentration of dye (ppm)

C_t- final concentration of dye (ppm)

3. Results and Discussion

3.1. Surface morphology analysis

The morphological images of the a) $BiVO_4$ and b) PPy-$BiVO_4$ nanocomposite were investigated using SEM as shown in Fig. 1. The $BiVO_4$ (image [a]) sample prepared at room temperature is looking like irregular particles which are aggregated. The close observation of $BiVO_4$ particles in pure sample indicates that they are composed of smaller primary crystals and size about 100 – 500 nanometers. The doping of polypyrrole over $BiVO_4$ will change the surface morphology. Inspection of SEM images suggests that particle growth has occurred in preferential direction from a common nucleus, yielding particles showing spherical size [7]. The results indicate that PPy doping can promote the growth of the particles and have significant influence on the morphology and microstructure of $BiVO_4$ samples.

From the EDX analysis, the atomic weight % of Bi and V ratio for $BiVO_4$ is 44.32 and 9.31. But the atomic weight % value of C, O, Cu, Pt, Sn, Bi, V and N ratio is 28.11, 12.38, 1.34, 1.01, 0.70, 43.60, 10.10 and 1.20 as shown in Fig.1 [c]. It shows that N-containing compound pyrrole was deposited on $BiVO_4$.

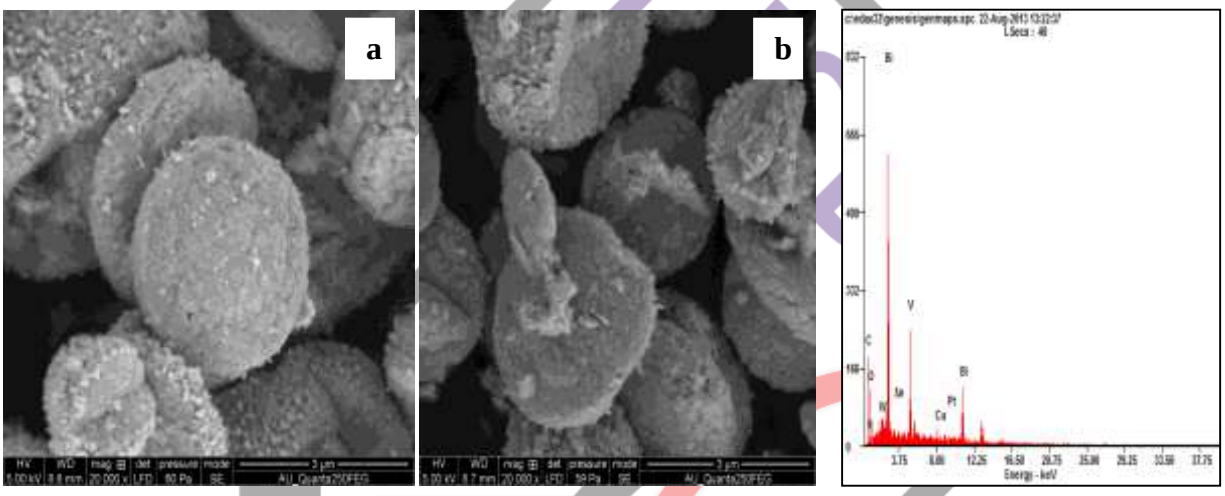

Fig. 1. SEM images of (a) $BiVO_4$ nanocomposite (b) PPy-$BiVO_4$ nanocomposite (c) EDAX spectrum for PPy-$BiVO_4$ nanocomposite

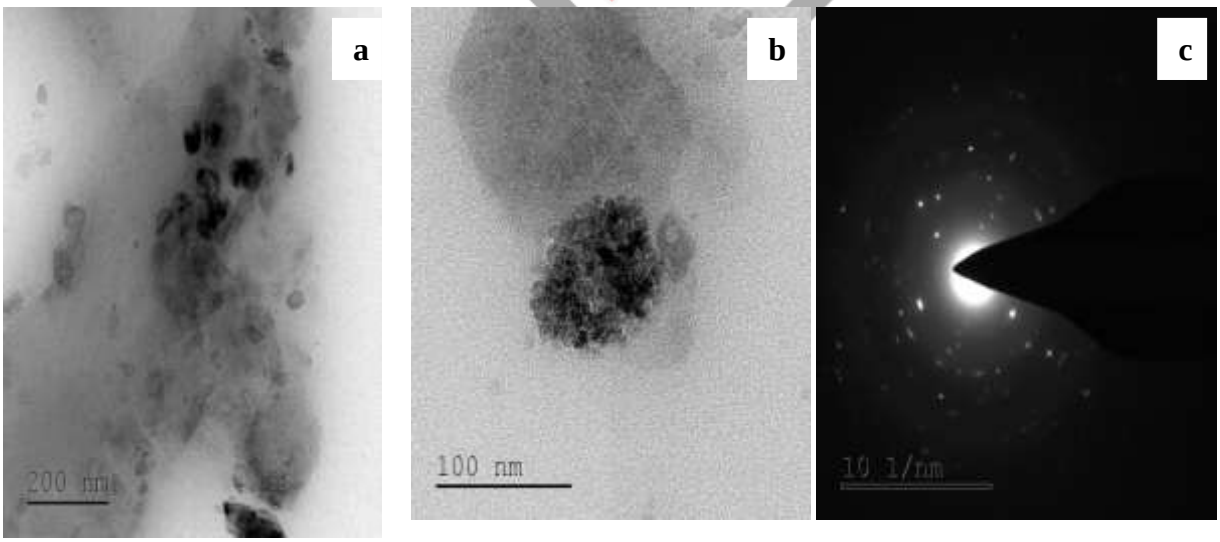

Fig .2 TEM images (a) PPy-$BiVO_4$ nanocomposite (b) $BiVO_4$ nanocomposite (c) SAED Pattern for PPy-$BiVO_4$ nanocomposite

The particle size and morphological investigation was carried out from TEM and it is presented in Fig. 2[a–c]. The TEM micrographs of PPy-$BiVO_4$ composite shows that $BiVO_4$ particles are dispersed on polypyrrole matrix (Figure. 2[a] and [b]

represents the highly close packed flower like structure of $BiVO_4$ particles which further confirmed the SEM observations. Fig.2[c] SAED pattern of PPy-$BiVO_4$ nanocomposite was investigated as shown in image [c] that shows the composite has a crystalline structure.

3.2. XRD analysis

The phase structure of the prepared material was measured by powder X-ray diffraction (XRD) analysis. The XRD pattern for the synthesized $BiVO_4$ and PPy-$BiVO_4$ nanocomposites are shown in Fig. 3. It can be seen that there is a difference between two curves in shape and position of the diffraction peaks. There is no diffraction peaks observed for PPy in PPy-$BiVO_4$ nanocomposite since it has small fraction of PPy.

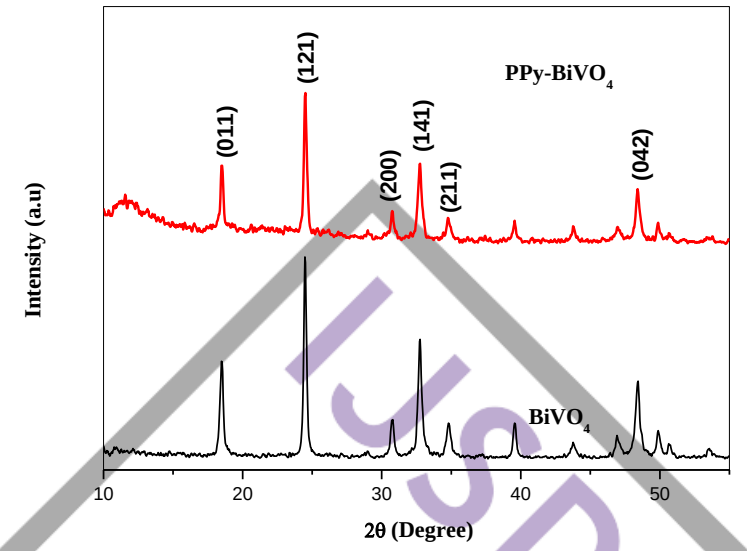

Fig. 3 XRD for PPy-$BiVO_4$ and $BiVO_4$ nanocomposite

The XRD peaks of pure $BiVO_4$ at 2θ of 18.98°, 35.45°, 39.9°, 47.2°, 50.26°, 53.7° were respectively indexed as (011), (002), (141), (240), (222), (310) [8-10]. The sharp peak at 2θ of 25.6° indicates polymer doping of PPy. It indicates the existence of smaller particle size in the nanocomposite containing high PPy content. Results imply that the crystalline phase of $BiVO_4$ has not been changed by the modification of PPy-$BiVO_4$. The mean sizes of $BiVO_4$ was calculated by Scherrer's formula,

$$D_{scherrer} = k\lambda/\beta \cos\theta \quad \text{----------} \quad (2)$$

Where, λ is the wavelength of the X-ray radiation ($\lambda = 1.54\times10^{-9}$nm)

k is the Scherrer constant (k =0.89)

θ is the diffraction angle and β is the line width at half-maximum height of the most intense peak. Based on the XRD results, the crystalline size of $BiVO_4$ and PPy-$BiVO_4$ nanocomposites are 7.92nm and 6.66nm respectively. These results are in good agreement with the SEM images.

3.3. UV-DRS studies

The optical band gap of crystalline $BiVO_4$ and PPy-$BiVO_4$ were estimated by UV-DRS spectra as shown in figure 4 that plot $(\alpha h\upsilon)^2$ *vs* photon energy showing the band gap value for the nanocomposite are 2.2eV and 2.75eV. It indicates that absorption edges of all PPy-$BiVO_4$ nanocomposites are quite similar to each other. The absorption band gaps corresponding to 400nm to 700nm were observed for pure $BiVO_4$ nanoparticles and PPy-$BiVO_4$ nanocomposites. Therefore, the PPy-$BiVO_4$ nanocomposite, enhanced the photocatalytic degradation activity in the visible light region is likely obtained. It can be seen that the polymer expands the absorption range of the PPy-$BiVO_4$ from 425 nm to 800 nm. It is observed that $BiVO_4$ has been deposited on the surface of Polypyrrole.

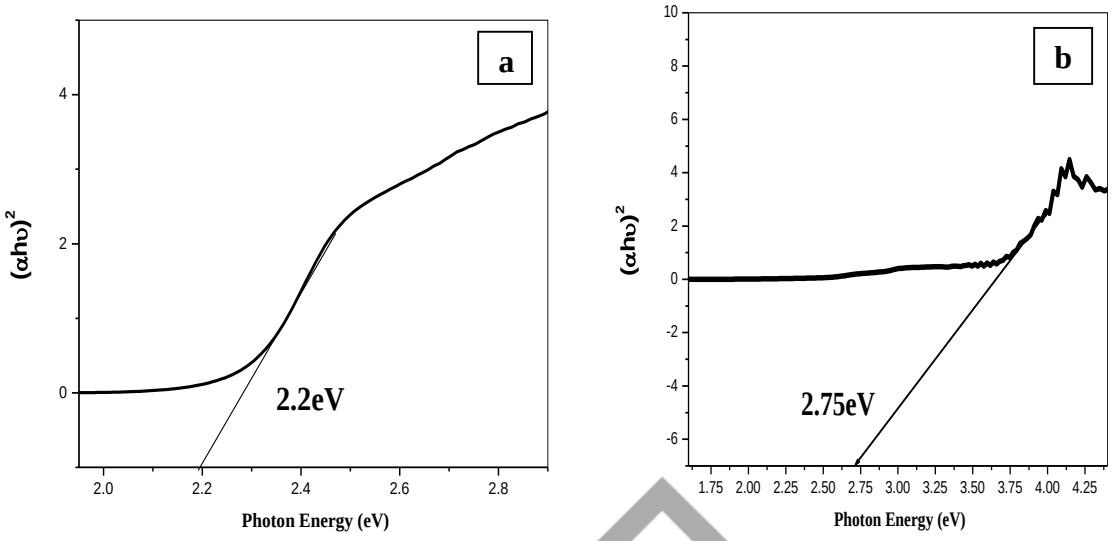

Fig . 4 Tauc Plot of the $(\alpha h\upsilon)^2$ vs photon energy ($h\upsilon$) for a) $BiVO_4$ and b) PPy-$BiVO_4$ nanocomposite

3.4. FT-IR studies

The FT -IR spectra of $BiVO_4$ and PPy-$BiVO_4$ nanocomposite are shown in Fig.5. The band 1400.2 cm^{-1} corresponds to the C-H plane vibration. The bands at 747.5 cm^{-1}, 987.4 $cm^{-1}$and 1100.1 cm^{-1} indicates the C-H wagging vibration. These bands represents the presence of polymer (polypyrrole). The broad pattern observed between 650 to 850 cm^{-1} consists of multiple characteristic bands which corresponds to the stretching and bending vibration bands of V-O and Bi-O [15-17].

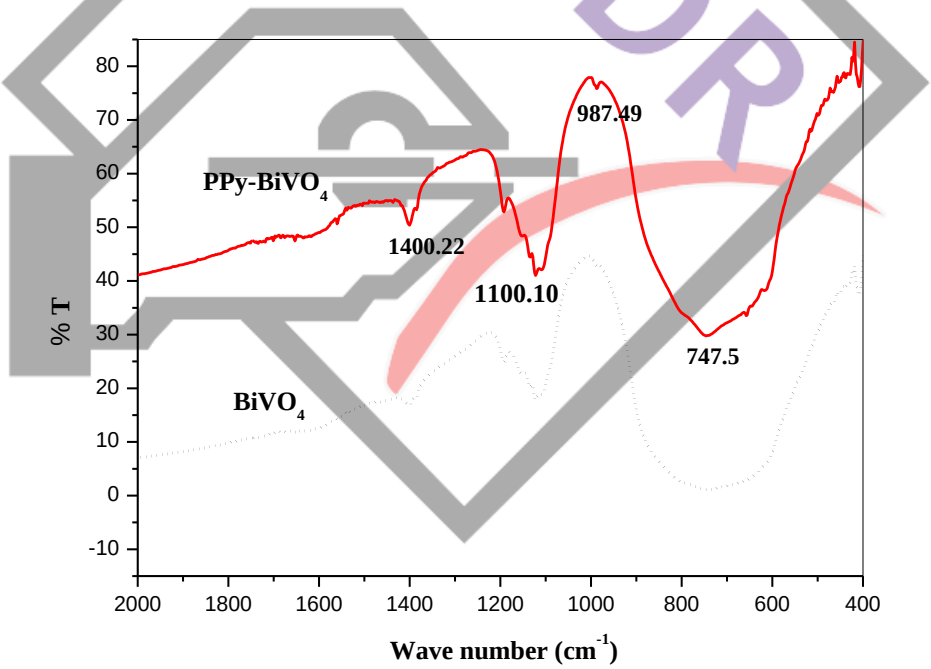

Fig. 5 FT-IR spectra for PPy-$BiVO_4$ and $BiVO_4$ nanocomposite

3.5. Photoluminescence studies

The photoluminescent (PL) spectra of PPy, $BiVO_4$ and PPy-$BiVO_4$ nanocomposites are shown in Fig.6. The emission wavelength peak is observed at 520 nm and shifted towards the blue. This emission is due to the recombination of electron and hole pairs. The absorption wavelength was observed at 380 nm and the difference between the absorption and emission peak wavelength is 140 nm indicating that the emission associated with the transition of electrons from trap state of conduction band. The PL studies show that the emission peak shifted towards the blue when compared to that of PPy-$BiVO_4$. The charge-transfer transition between vanadium 3d and oxygen 2p orbital inVO_4^{3-} and the peak 520 nm corresponds to the charge transfer involving Bi and V centers. This result suggests that the combination of PPy and $BiVO_4$ heterostructures facilitates the efficient separation of photogenerated carriers

leading to enhanced photocatalytic activity [18-20]. The PL results are in agreement with the analysis done according to the proposed scheme 1.

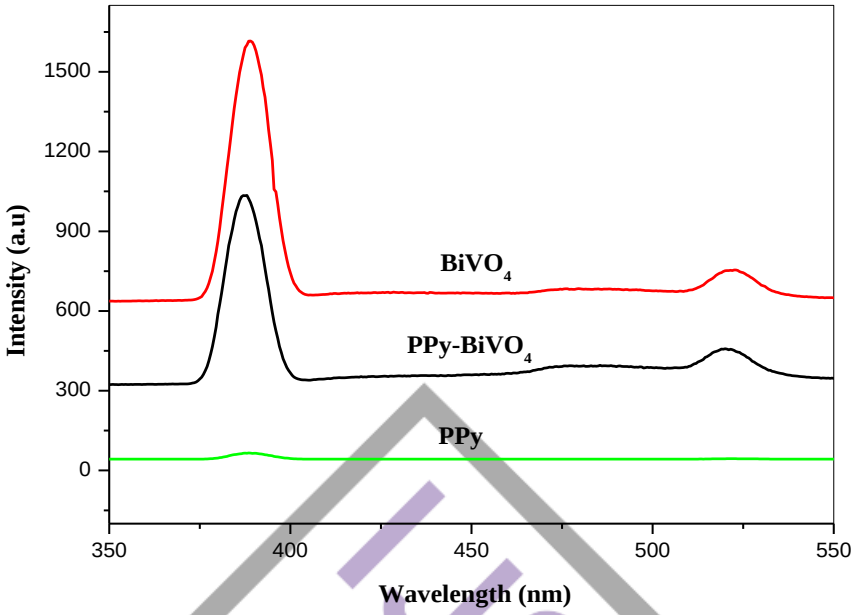

Fig.6 PL spectra for PPy, $BiVO_4$ and PPy-$BiVO_4$ nanocomposite

3.7. Thermogravimetric Analysis

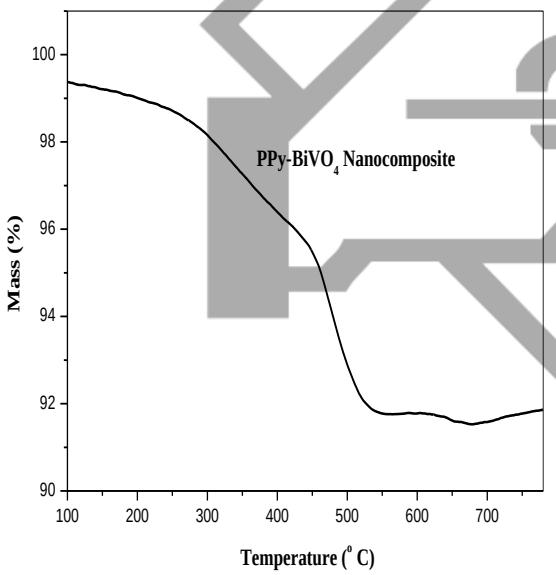

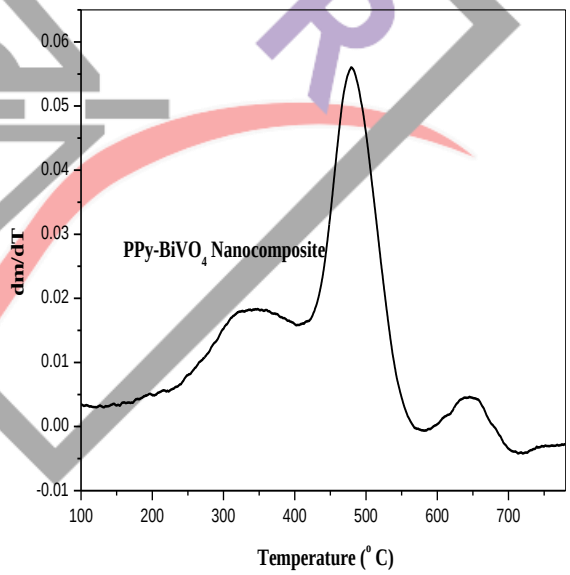

Fig. 7 TGA spectrum for PPy- $BiVO_4$ nanocomposite **Fig.8** DTA spectrum for PPy- $BiVO_4$ nanocomposite

The thermogram also provides additional information about the composition of the oxidation products. Fig. 7 indicates two major stages of weight loss. The first decomposition at 120°C corresponds to the removal of water molecules from the surface of the composite. This is followed by a continuous weight loss (TGA) upto 505°C which could denote the combustion of the organic polymer component. This is in agreement with the DTA curve where a large, relatively sharp exothermic peak at 200 to 310°C is distinct due to the oxidation of the PPy [21-22]. Furthermore, the weight loss from TGA curve at 740°C is in agreement with the DTA curve of a relatively sharp endotherm at 780°C, due to the melting of $BiVO_4$ present in the nanocomposite as shown in Fig.8.

3.8. Mechanism

The possible photocatalytic mechanism is shown in scheme.1. PPy as a conducting polymer with an extended conjugated electron system has recently showed great promises due to its high absorption coefficients in the visible light range and high mobility of charge carriers. PPy is a good material for transporting holes. On the basis of the relative energy level of PPy and $BiVO_4$, which leads to synergic effect, the photogenerated holes in the valence band (VB) of $BiVO_4$ can directly be transferred to the orbital of PPy. Simultaneously, the photogenerated electrons transfer to the conduction band (CB) of $BiVO_4$, which results in charge separation and stabilization.

3.9. Zero point charge

The aqueous suspension of adsorbent material (100mg in 50ml) is prepared in 50 ml solution of $NaNO_3$ of concentration 0.001N. Aliquots of suspension are adjusted to various pH values by using dilute solution of sodium hydroxide and Nitric acid of strength 1.0 N. After it is shaken for 60 min, in a thermostatic mechanical orbit shaker, The pH value (initial pH) is measured with a pen type digital pH meter. Then, one gram of sodium nitrate is added to aliquot in each bottle, to bring a final electrolyte concentration to about 0.45 M. After an additional 60 min agitation, the final pH is measured with pen type digital pH meter. The ΔpH (ΔpH = Final pH – Initial pH) is calculated and plotted against solution pH. Typical plots of ΔpH Vs pH of the solution are obtained for the determination of zero point charge (pH_{zpc}). The pH at which the ΔpH = 0, yielded pH_{ZPC} value. The zero point charge for the synthesised PPy-$BiVO_4$ nanocomposite is 3.0 [23-24].

4. Photodegradation studies

The Photocatalytic activities of the PPy–$BiVO_4$ nanocomposites were evaluated by monitoring the photodegradation of Methylene Blue (MB).

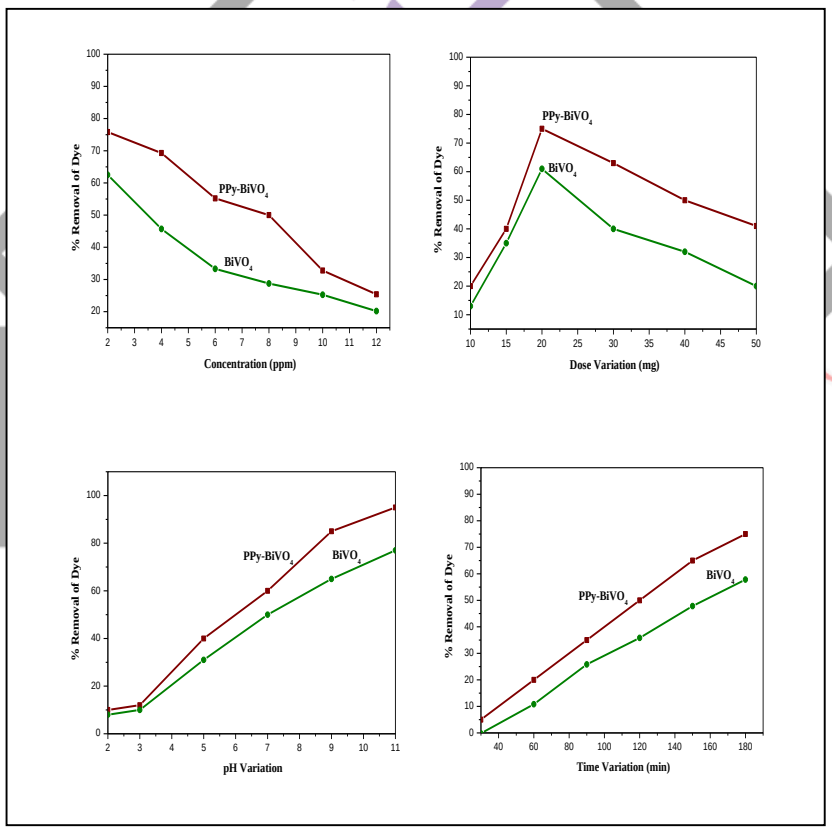

Fig. 9 Effect of Various operational Parameters a) Concentration b) Dose of Catalyst c) pH Variation d) Time Variation on the photodegradation of MB dye on PPy- $BiVO_4$ nanocomposite and $BiVO_4$

4.1. Effect of the initial dye concentration

The initial concentration of dye solution increases from 2ppm to 12ppm. The percentage removal of dye obtained 75.8% for PPy-$BiVO_4$ and 62.5% for $BiVO_4$ nanocomposites. When dye concentration increases more number of organic substances (dye molecules) are adsorbed on the surface of catalyst, they reduced the hydroxyl radicals generation. Further, as the concentration of a dye solution increases, the photons get intercepted before they can reach the catalyst surface, hence the absorption of photons by the catalyst decreases, and consequently the degradation percent is reduced [25–27] as shown in Fig.9a. Concentration of intermediates formed and absorption of photons by dye and intermediates increases at higher dye concentration resulting in lesser energy available for hydroxyl generation [28].

4.2. Effect of photocatalyst loading

The increase of catalyst loading beyond the optimum may result in the agglomeration of catalyst particles, hence the part of the catalyst surface become unavailable for photon absorption and degradation rate decreases. When the catalyst loaded at 0.050g, the photodegradation efficiency abruptly decreased to 41% and 20% for both PPy-$BiVO_4$ and $BiVO_4$ nanocomposites. This is due to an agglomeration and sedimentation of the catalyst particles which caused an increase in the particle size and decrease in specific surface area which lead to decrease in the number of surface active sites. Also at high amount of catalyst, the opacity, turbidity of the suspension, and light scattering of catalyst particles are increased. This tends to decrease the passage of irradiation through the sample. Therefore, the most effective photodegradation for methylene blue is observed with 0.020g of catalyst-loading dose [29-30] as shown in Fig.9b.

4.3. Effect of pH variation

The effect of pH on the photocatalytic degradation of MB dye studied by varying the initial pH of MB dye solution varies from 2 to 11 and keeping constant for all other experimental parameters constant. The percentage of photocatalytic decolorization considerably increases with increase in pH of the catalysts. The % removal of dye molecules depends upon the zero point charge of the catalyst. The zero point charge for the synthesised PPy-$BiVO_4$ was 3.0. Under acidic pH (< 3), the catalyst surface will be positively charged and contains more surface active sites. The Lewis base property of MB dye renders the molecule to get adsorbed more easily on the catalyst surface. The presence of negatively charged acidic sulfonate group drives the MB dye molecule to adsorb strongly on catalyst surface and hence undergoes faster degradation as shown in Fig.9c. The interpretation of pH effects on the degradation process is rather complex as it includes several factors such as (i) electrostatic interaction between the catalyst surface and the dye molecules; (ii) reaction of superoxide and hydroxyl radicals formed on the catalyst surface with the dyes; (iii) concentration of hydroxyl radical generation [31-36].

4.4. Effect of time variation

The percentage of dye degradation increases with increase in irradiation time and complete degradation was obtained with 180 minutes as shown in Fig.9d. This may be due to an increase in irradiation time. The dye molecules and catalysts have enough time to take part in photocatalytic degradation process and hence percentage of degradation increases [37-43].

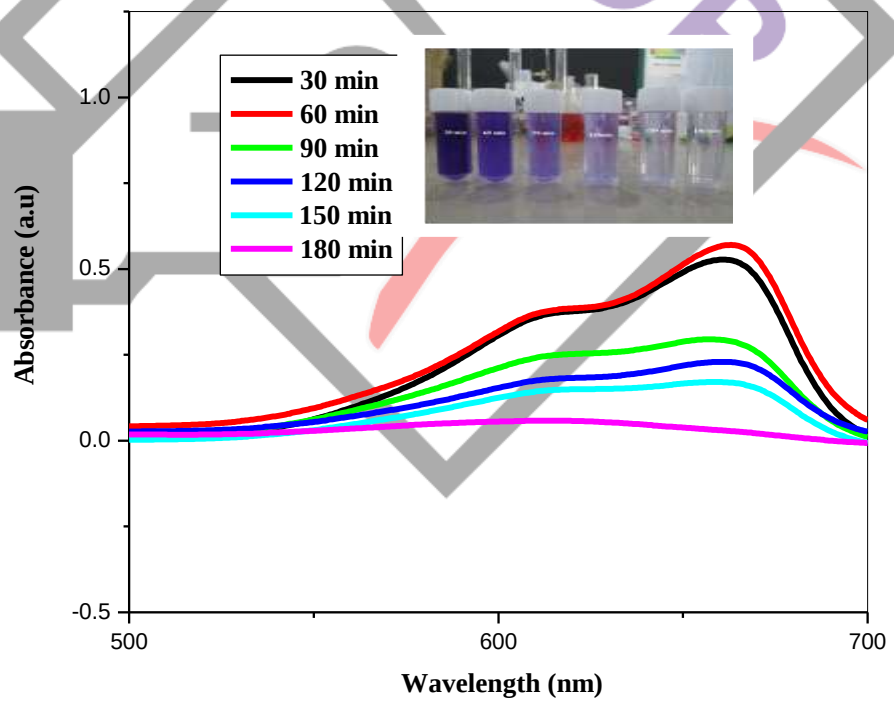

Fig . 10 UV-vis absorption spectra of MB dye degradation using PPy-$BiVO_4$ nanocomposite under Sun light with different intervals of time [30, 60, 90, 120, 150, 180]

Fig.10 depicts the UV-vis absorption spectrum of MB dye degradation in the presence of PPy-$BiVO_4$ nanocomposite under sun light irradiation. Sunlight irradiation leads to a continuous decrease in absorbance of MB dye in the presence of PPy-$BiVO_4$ nanocomposite and the decrease of the absorption band intensities of the dye indicated that dye has been degraded.

The decoloration kinetics of MB dye by using Sunlight irradiation was investigated with PPy-$BiVO_4$ and $BiVO_4$ nanocomposites. The results showed that the photocatalytic degradation of MB dye obey apparently pseudo first order kinetics and the rate expression is given by the following equation.

$$ln\left(\frac{Co}{Ct}\right) = kt \quad ---------- \quad (3)$$

Where,
C_o = initial concentration of dye solution (in ppm)
C_t = final concentration of dye solution in various time interval (in ppm)
k = pseudo-first order rate constant for degradation of dye (in min^{-1})
t = irradiation time respectively.
The value of ln (Co/Ct) is plotted against time (in min.) and the plots are found to be linear as shown in Fig.11.

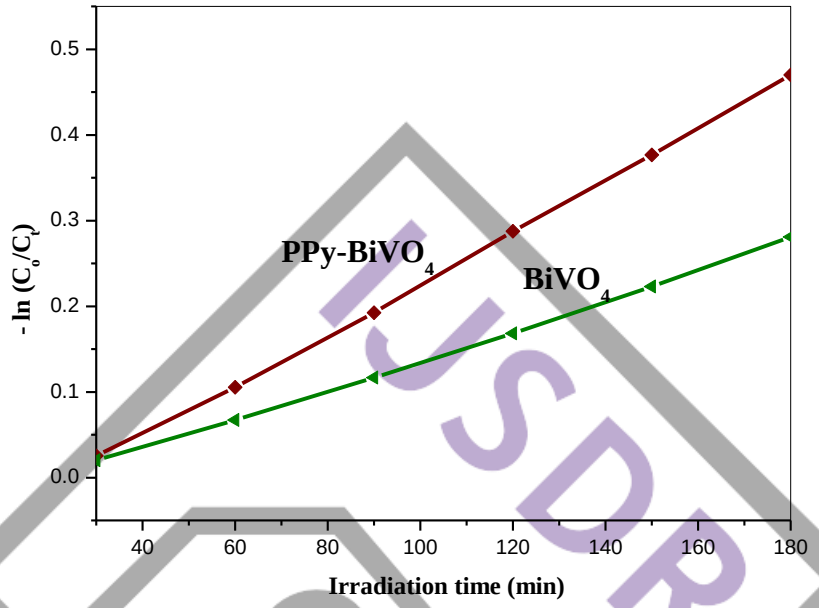

Fig. 11 Apparent first-order linear transforms – ln (C_0/C_t) vs. t of MB dye (dye concentration : 2ppm) and (catalyst dose : 0.4g/L^{-1})

Hence, the development of photocatalysts is capable of absorbing light in the visible region of the spectrum. The degradation rate constant values of PPy-$BiVO_4$ and $BiVO_4$ nanocomposite under sunlight system are k= 0.0066 min^{-1} and k= 0.0039 min^{-1}. The enhanced activity might be mainly attributed to the role of PPy played an improvement in light-harvesting ability in sunlight and as electron acceptor-transporter in the composite, which effectively suppressed the charge recombination and promoted the charge transfer within $BiVO_4$.

4.5. Composite recovery

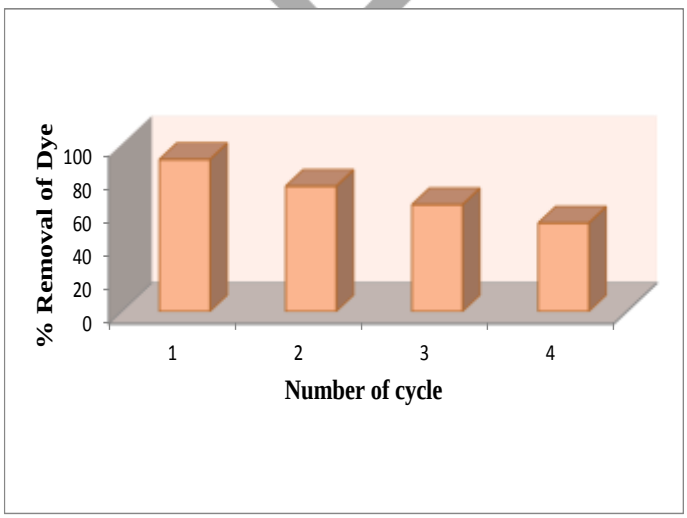

Fig.12 Reuse of Catalyst

0.02g of composite was used to degrade 2ppm solution under sunlight for 180 min. The degradation rate is almost the best value of 90 %. The composite was therefore reused to observe the degradation under this condition. The degradation rate is 75% in the second use. In the third and fourth reuse, the percentage degradation are 75 and 57. It is shown in Fig.12. This shows that photocatalytic activity of the composite is still good enough for recycle [44-45].

4.6 Anti microbial activity

Antimicrobial activity of the prepared PPy-$BiVO_4$ was determined by agar diffusion method on nutrient agar medium. The microbial strains like E.coli maintained on sterile nutrient agar at 3- 4º C. A loop of innoculum was transferred into 5ml of nutrient broth and incubated at 2hrs at 37ºC. 1ml of these sample was spread on nutrient agar plate. Then, 4 wells were made in sterile nutrient agar plate corkborer. Then 50µl of solvent containing nanocomposite was placed in the wells made in nutrient agar plate. The treatment also includes as penicillin as positive control. The plate was incubated for 24hrs at 37ºC and the zone of inhibition around the well was measured by -----mm. The effect of the material on bacteria have been studied by many research papers. In the present work, two different samples were used for antibacterial activity. The activity of PPy-$BiVO_4$ was higher against E.Coli bacteria than compared to $BiVO_4$.[46-47].

Acknowledgement

We thank the UGC, New Delhi for providing financial support for our research work.

References

[1] V. Eskizeybek, F. Sarı, H. Gulce , A. Gulce, A. Avcı, Preparation of the new polyaniline/ZnO nanocomposite and its photocatalytic activity for degradation of methylene blue and malachite green dyes under UV and natural sun lights irradiations, Appl. Catal. B Environ.119– 120 (2012) 197– 206.
[2] F. Deng, Y. Li, X. Luo, L. Yang, X. Tu, Preparation of conductive polypyrrole/TiO_2 nanocomposite via surface molecular imprinting technique and its photocatalytic activity under simulated solar lightirradiation, Colloids and Surfaces A: Physicochem. Eng. Aspects 395 (2012) 183– 189
[3] W. Sun, J. Li, G. Yao, F. Zhang, J. Wang, Surface-modification of TiO_2 with new metalloporphyrins and their photocatalytic activity in the degradation of 4-notrophenol, Appl. Sur. Sci. 258 (2011) 940– 945
[4] X. Zhang, Z. Ai, F. Jia , L. Zhang, X. Fan, Z. Zou, Selective synthesis and visible-light photocatalytic activities of $BiVO_4$ with different crystalline phases, Mater. Chem. Phy. 103 (2007) 162–167
[5] S. Xie, T. Zhai, Y. Zhu, W. Li , R. Qiu,Y. Tong, X. Lu, NiO decorated Mo:$BiVO_4$ photoanode with enhanced visible-light photoelectrochemical activity, Int. J. Hydrog. Energy 39 (2014) 4820- 4827
[6] L. Zhang, G. Tan, S. Wei, H. Ren, A. Xia, Y. Luo, Microwave hydrothermal synthesis and photocatalytic properties of TiO_2/$BiVO_4$ composite photocatalysts, Ceram. Int. 39 (2013) 8597–8604.
[7] N.R. Khalid, E. Ahmed, Z. Hong, M. Ahmad, Y. Zhang, S. Khalid, Cu-doped TiO_2 nanoparticles/graphene composites for efficient visiblelight photocatalysis, Ceram. Int. 39 (2013) 7107–7113
[8] M.Sangareswari, M.Meenakshi Sundaram, A Comparative Study on Photocatalytic Efficiency of TiO_2 and $BiVO_4$ Nanomaterial for Degradation of Methylene Blue Dye under Sunlight Irradiation, J.Adv. Chem.Sci 1 (2) (2015) 75-77
[9] M.Meenakshi Sundaram, M.Sangareswari, P.Muthirulan, Enhanced Photocatalytic Activity of Polypyrrole/TiO_2 Nanocomposites for Acid Violet Dye Degradation under UV Irradiation, IJIRSE 2 (2014) 420-423
[10] L. Gomathi Devi, S. Girish Kumar, Exploring the critical dependence of adsorption of various dyes on the degradation rate using Ln3þ–TiO_2 surface under UV/solar light, Appl. Surf. Sci. 261 (2012) 137–146.
[11] S.Q.Wang, Q.L.Liu, A.M.Zhu, Preparation of multisensitive poly (N-isopropylacrylamide-co-acrylic acid)/TiO_2 composites for degradation of methyl orange, Eur. Poly. Journal 47 (2011) 1168–1175
[12] D. Wang, J. Zhang, Q. Luo, X. Li, Y. Duan, J. An, Characterization and photocatalytic activity of poly(3-hexylthiophene)-modified TiO_2 for degradation of methyl orange under visible light, J. Hazar. Mater .169 (2009) 546–550
[13] A.R. Khataee, M.B. Kasiri, Photocatalytic degradation of organic dyes in the presence of nanostructured titanium dioxide: Influence of the chemical structure of dyes, J. Mol. Catal A: Chem. 328 (2010) 8–26
[14] L. Gu, J. Wang, R. Qi, X. Wang, P. Xu, X. Han, A novel incorporating style of polyaniline/TiO_2 composites as effective visible photocatalysts, J. Mol. Catal A: Chem 357 (2012) 19– 25
[15] R. Venkatesan, S. Velumani , A. Kassiba, Mechanochemical synthesis of nanostructured $BiVO_4$ and investigations of related features, Mater. Chem. Phy. 135 (2012) 842-848
[16] S. Dong, J. Feng, Y. Li, L. Hu, M. Liu, Y. Wang , Y. Pi, J. Sun, J. Sun, Shape-controlled synthesis of $BiVO_4$ hierarchical structures with unique natural- sunlight- driven photocatalytic activity, Appl. Catal B: Environ. 152–153 (2014) 413–424
[17] J. Savio, A. Moniz , J. Zhu , J. Tang , 1D Co-Pi Modified $BiVO_4$ /ZnO Junction Cascade for Efficient Photoelectrochemical Water Cleavage, Adv. Energy Mater. 4 (2014) 1-8
[18] C. Ravidhas , A. J. Josephine, P. Sudhagar , A. Devadoss, C. Terashima, K. Nakata , A. Fujishima, A. Ezhil Raj, C. Sanjeeviraja, Facile synthesis of nanostructured monoclinic bismuth vanadate by a co-precipitation method: Structural, optical and photocatalytic properties, Mater. Sci. Semi. Process. 30 (2015) 343–351
[19] S. Obregón,S.W. Lee, G. Colón, Exalted photocatalytic activity of tetragonal $BiVO_4$ by Er^{3+} doping through a luminescence cooperative mechanism†, Dalton Trans. 43 (2014) 311-316

[20] R.Bajaj, M.Sharma, D.Bahadur, Visible light-driven novel nanocomposite ($BiVO_4/CuCr_2O_4$) for efficient degradation of organic dye†, Dalton Trans. (2013) 1-9
[21] Y. Zhu, Y. Liu, Y. Lv,Q. Ling,D. Liu, Y. Zhu, Enhancement of photocatalytic activity for $BiPO_4$ via phase junction†, J. Mater. Chem. A, 2 (2014) 13041–13048
[22] C. E. Corcione, M. Frigione, Characterization of Nanocomposites by Thermal Analysis, Materials 5 (2012) 2960-2980
[23] H. S. Park , H.W.Ha , R. S. Ruoff, A.J. Bard, On the improvement of photoelectrochemical performance and finite element analysis of reduced graphene oxide–$BiVO_4$ composite electrodes, J. Electroanal. Chem. 716 (2014) 8–15
[24] F. Zhang, J. Zhaoa, T. Shen, H. Hidaka, E. Pelizzettic, N. Serpone, TiO_2- assisted photodegradation of dye pollutants II. Adsorption and degradation kinetics of eosin in TiO_2 dispersions under visible light irradiation, Appl. Catal B: Environ 15 (1998) 147-156.
[25] A.Giwa , P. O. Nkeonye, K. A.Bello, K. A.Kolawole, Photocatalytic Decolourization and Degradation of C. I. Basic Blue 41 Using TiO_2 Nanoparticles, J. Environ. Protect. 3 (2012) 1063-1069
[26] S.K. Kansal, N. Kaur, S. Singh, Photocatalytic degradation of two commercial reactive dyes in aqueous phase using nanophotocatalysts, Nanoscale Res. Lett. 4 (2009) 709–716.
[27] A. Akyol, H.C. Yatmaz, M. Bayramoglu, Photocatalytic decolorization of Remazol Red RR in aqueous ZnO suspensions, Appl. Catal. B Environ. 54 (2004) 19–24.
[28] M.A. Behnajad. N. Modirshahla. N. Daneshva. and M. Rabbani., Photo catalytic degradation of an azo dye in a tubular continuous-flow photo reactor with immobilized TiO_2 on glass plates, Chem. Eng. Journ. 127 (2007) 167–176
[29] C.C. Chen. C.S.Lu. Y.C.Chung. and J.L Jan., UV light induced photo degradation of malachite green on TiO_2 nanoparticles, J. Hazar. Mater.141 (2007) 520– 528
[30] H. Liu, X. Dong, C. Duan, X. Su, Z. Zhu, Silver-modified TiO_2 nanorods with enhanced photocatalytic activity in visible light region, Ceram. Int. 39 (2013) 8789–8795.
[31] P.Muthirulan,C.NirmalaDevi,M.Meenakshi Sundaram,TiO_2wrapped grapheneasahighperformancephotocatalystforacidorange 7 dye degradationundersolar/UV light irradiations, Ceram. Int. 40 (2014) 5945–5957
[32] T. A. Kandiel, R.Dillert, D. W. Bahnemann, Enhanced photocatalytic production of molecular hydrogen on TiO_2 modified with Pt–polypyrrole nanocomposites†, Photochem. Photobiol. Sci., 8 (2009) 683–690
[33] Y. Zhu,Y. Dan, Photocatalytic activity of poly(3-hexylthiophene)/titanium dioxide composites for degrading methyl orange, Sol. Energy. Mater. & Solar Cells 94 (2010) 1658–1664
[34] X. Huang, G. Wang, M.Yang, W. Guo, H. Gao, Synthesis of polyaniline-modified $Fe_3O_4/SiO_2/TiO_2$ composite microspheres and their photocatalytic application, Mater. Lett. 65 (2011) 2887-2890
[35] A.K.M. Fung, B. K.W. Chiu, M.H.W. Lam, Surface modification of TiO_2 by a ruthenium(II) polypyridyl complex via silyl-linkage for the sensitized photocatalytic degradation of carbon tetrachloride by visible irradiation, Water Research 37 (2003) 1939–1947
[36] M. Stylidi, D. I. Kondarides, X. E. Verykios, Visible light-induced photocatalytic degradation of Acid Orange 7 in aqueous TiO_2 suspensions, Appl. Catal B: Environ. 47 (2004) 189–201
[37] H.M. Pinheiro, E. Touraud, O. Thomas, Aromatic amines from azo dye reduction: status review with emphasis on direct UV spectrophotometric detection in textile industry wastewaters, Dyes and Pigments 61 (2004) 121–139
[38] H.Chun, W.Yizhong, T.Hongxiao, Influence of adsorption on the photodegradation of various dyes using surface bond-conjugated TiO_2/SiO_2 photocatalyst, Appl.Catal.B: Environ. 35 (2001) 95–105
[39] B.J.P.A Cornish, L.A. Lawton, P.K.J. Robertson, Hydrogen peroxide enhanced photocatalytic oxidation of microcystin-LR using titanium dioxide, Appl.Catal.B: Environ. 25 (2000) 59–67
[40] T. C.-K. Yang, S.F.Wang, S.H.Y. Tsai, S.Y. Lin, Intrinsic photocatalytic oxidation of the dye adsorbed on TiO_2 photocatalysts by diffuse reflectance infrared Fourier transform spectroscopy, Appl Catal B: Environ 30 (2001) 293–301
[41] I.K. Konstantinou, V.A. Sakkas, T. A. Albanis, Photocatalytic degradation of the herbicides propanil and molinate over aqueous TiO_2 suspensions: identification of intermediates and the reaction pathway, Appl Catal B: Environ. 34 (2001) 227–239
[42] S. Parra, J. Olivero, L. Pacheco, C. Pulgarin, Structural properties and photoreactivity relationships of substituted phenols in TiO_2 suspensions, Appl. Catal B: Environ. 43 (2003) 293–301
[43] L.A. Lawton, P.K.J. Robertson, R.F. Robertson, F. G. Bruce, The destruction of 2-methylisoborneol and geosmin using titanium dioxide photocatalysis, Appl.Catal B: Environ. 44 (2003) 9–13
[44] P.Esparza, M.E. Borges, L. Díaz, M.C. Alvarez-Galván, J.L.G. Fierro, Photodegradation of dye pollutants using new nanostructured titania supported on volcanic ashes, Appl. Catal. A: Gen. 388 (2010) 7–14
[45] M.Sangareswari, M.Meenakshi Sundaram, Development of efficiency improved polymer-modified TiO_2 for the photocatalytic degradation of an organic dye from wastewater environment, Appl.Water.Sci. 351 (2015) 1-12
[46] W. Wang, Y. Yu, A.Taichang, L. Guiying, Y. Yip, J.C. Yu, P. K. Wong Visible-Light-Driven Photocatalytic Inactivation of *E. coli* K-12 by Bismuth Vanadate Nanotubes: Bactericidal Performance and Mechanism Environ. Sci. Technol., 2012, 46 (8), pp 4599–4606
[47] W. Wang, G. Huang, J. C.Yu, P. KeungWong, Advances in photocatalytic disinfection of bacteria: Development of photocatalysts and mechanisms, Journal of environmental science, 34, 2015, 232-247